

ANTS: Shaping the Adaptive Negative Textual Space by MLLM for OOD Detection

Zhu Wenjie^{1,2*} Zhang Yabin^{3*} Xin Jin² Wenjun Zeng^{2†} Lei Zhang^{1†}

¹The Hong Kong Polytechnic University ²Eastern Institute of Technology, Ningbo

³Stanford University

22040319r@connect.polyu.hk, wzeng-vp@eitech.edu.cn, cslzhang@comp.polyu.edu.hk

Github page: <https://github.com/ZhuWenjie98/ANTS>

Abstract

The introduction of negative labels (NLs) has proven effective in enhancing Out-of-Distribution (OOD) detection. However, existing methods often lack an understanding of OOD images, making it difficult to construct an accurate negative space. In addition, the presence of false negative labels significantly degrades their near-OOD performance. To address these issues, we propose shaping an Adaptive Negative Textual Space (ANTS) by leveraging the understanding and reasoning capabilities of multimodal large language models (MLLMs). Specifically, we identify images likely to be OOD samples as negative images and prompt the MLLM to describe these images, generating expressive negative sentences that precisely characterize the OOD distribution and enhance far-OOD detection. For the near-OOD setting, where OOD samples resemble the in-distribution (ID) subset, we first identify the subset of ID classes that are visually similar to negative images and then leverage the reasoning capability of MLLMs to generate visually similar negative labels tailored to this subset, effectively reducing false negatives and improving near-OOD detection. To balance these two types of negative textual spaces, we design an adaptive weighted score that enables the method to handle different OOD task settings (near-OOD and far-OOD) without relying on task-specific prior knowledge, making it highly adaptable in open environments. On the ImageNet benchmark, our ANTS significantly reduces the FPR95 by 4.2%, establishing a new state-of-the-art. Furthermore, our method is training-free and zero-shot, enabling high scalability.

1. Introduction

Deep neural networks (DNNs) have achieved remarkable performance in classifying test samples that fall into the training distribution [16, 21, 34]. However, it is well-known

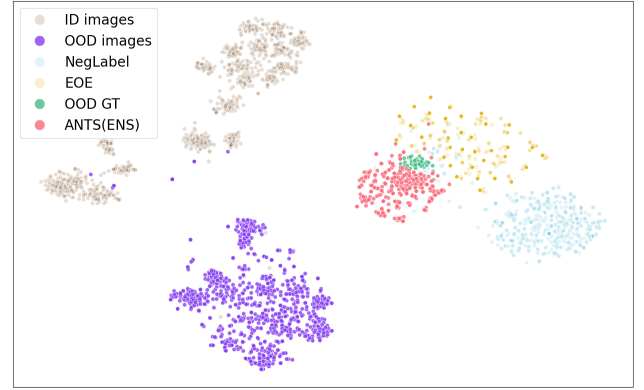


Figure 1. T-SNE visualization of the ID and OOD image features, the text features of NegLabel [31], EOE [6], OOD ground-truth, and the expressive negative sentences (ENS) of ANTS. We select ImageNet and SUN as the ID and OOD datasets, respectively. NegLabel and EOE lack a good understanding of OOD images, resulting in a greater distance between the OOD images and the text features. In contrast, our ANTS utilizes the MLLMs to understand OOD images during ENS generation, reducing the distance between ENS and OOD images and improving OOD detection performance.

that DNNs tend to misclassify test samples from unknown classes, which are often called out-of-distribution (OOD) data [22]. Unfortunately, OOD data are inevitably encountered in open environments. Therefore, how to effectively identify OOD data is crucial for the reliable deployment of DNN models in open-world scenarios.

Traditional OOD detection methods in the image domain primarily rely on visual modality information [25, 27, 63, 70, 73]. For example, MSP [22] utilizes the maximum softmax probability of a pre-trained vision model to detect OOD images. Recently, multimodal knowledge has attracted increasing attention in OOD detection [4, 32, 42, 48, 51, 53, 78, 84, 85]. In particular, NegLabel [32] introduces negative labels (NLs) by mining words that are semantically distant from in-distribution (ID) labels, and identifies OOD images

*These authors contributed equally to this work.

†Corresponding authors.

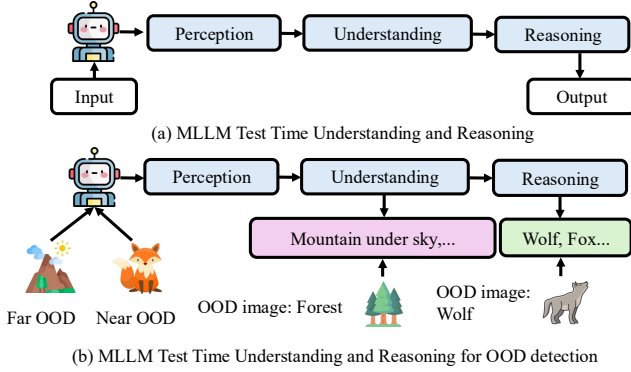


Figure 2. (a) Current MLLM improve their reasoning abilities by test time understanding and reasoning through chain-of-thought (CoT) prompting. (b) In our work, we leverage the test time understanding and reasoning capabilities of MLLM during inference to help visual-language models perform better on OOD detection.

by comparing their similarities to NLs and ID labels. Similar approaches generate NLs by prompting LLMs [6] or modifying superclass names [8]. Although these methods have achieved promising performance, they suffer from three key limitations. First, due to the lack of understanding of OOD images, the NLs are positioned far from the OOD image, as illustrated in Fig. 1. Second, these methods struggle with the challenging near-OOD setting, where OOD samples are semantically close to ID labels. NegLabel focuses on generating NLs that are semantically distant from ID classes, inherently overlooking such cases. While EOE [6] introduces visually similar labels for all ID classes to address this problem, it neglects the fact that OOD samples are typically similar to only a subset of ID classes, resulting in many false negative labels (see Fig. 6a). Third, these methods rely on the strong assumption that the target task setting (*e.g.*, near OOD or far OOD) is known in advance, allowing for the tailored design of NL generation rules. However, this assumption limits their applicability in complex, unknown, and dynamically changing open environments.

To address these challenges, we propose to shape an Adaptive Negative Textual Space (ANTS) by harnessing the understanding and reasoning capabilities of multimodal large language models (MLLMs) [2, 3, 39, 45], as shown in Fig. 2. Specifically, we introduce expressive negative sentences (ENS), which effectively capture fine-grained details of OOD images. These negative sentences are generated by prompting MLLMs to describe online-mined negative images, leveraging their multimodal understanding capabilities and significantly enhancing the traditional far-OOD detection. While ENS shows greater expressive power in identifying far-OOD samples, it faces challenges in handling the near-OOD setting, where OOD samples are semantically close to certain ID classes. To address this, we dynamically identify the subset of ID classes most similar to the negative images and utilize the reasoning capabilities of MLLMs to

construct visually similar negative labels (VSNL) tailored for this subset. This targeted approach reduces false negative labels and improves performance in the near-OOD setting (see Fig. 6a). Finally, to ensure adaptability across diverse task settings in open environments, we introduce an adaptive weighted score function to balance the two distinct negative textual spaces. This dynamic mechanism enables the model to seamlessly handle both near-OOD and far-OOD scenarios without prior knowledge of the task settings. The overall framework is presented in Fig. 3.

We conduct extensive experiments to validate the advantages of our ANTS method. On the large-scale ImageNet dataset, our approach significantly reduces FPR95 by 4.2% and 3.25% in the far-OOD and challenging near-OOD detection settings, respectively. Moreover, our method operates in a zero-shot and training-free manner, demonstrating strong scalability across different MLLMs. We summarize our contributions as follows:

- We identify three limitations of existing NLs-based methods: (1) lack understanding of OOD images; (2) struggle to address the challenging near-OOD setting, where OOD samples are semantically close to ID labels; (3) rely on the strong assumption that the target task setting (*e.g.*, near-OOD or far-OOD) is known in advance.
- To overcome these limitations, we propose the ANTS approach by leveraging the understanding and reasoning capabilities of MLLMs. Specifically, we (1) design two types of prompt for MLLMs to generate expressive negative sentences and visually similar negative labels; (2) introduce two strategies including Negative Images Mining and Visually Similar ID-Classes Mining to avoid interference from ID noise and generate false negative labels; and (3) design an adaptive weighted score to dynamically balance these two text spaces in open environments.
- Extensive experiments are conducted to validate the proposed components. Our method demonstrates new state-of-the-art performance on both near-OOD and far-OOD detection tasks, achieving significant gains without any prior knowledge about the task setting.

2. Related Work

Traditional OOD Detection. Traditional OOD detection methods can be categorized into the following groups: (1) classification-based methods [15, 19, 22, 23, 26, 31, 36, 43, 44, 46, 49, 54, 55, 60, 62, 63, 66, 74, 79, 80, 83] that distinguish ID and OOD samples by designing a score function; (2) density-based methods [1, 28, 56, 58, 71, 89] that detect OOD samples by evaluating the likelihood or density of test data derived from probabilistic models; (3) distance-based methods [50, 67, 81] that classify test samples as OOD if they deviate significantly from the prototypes of in-distribution classes; (4) reconstruction-based methods [13, 29, 38, 76, 87] that focus on detecting OOD samples

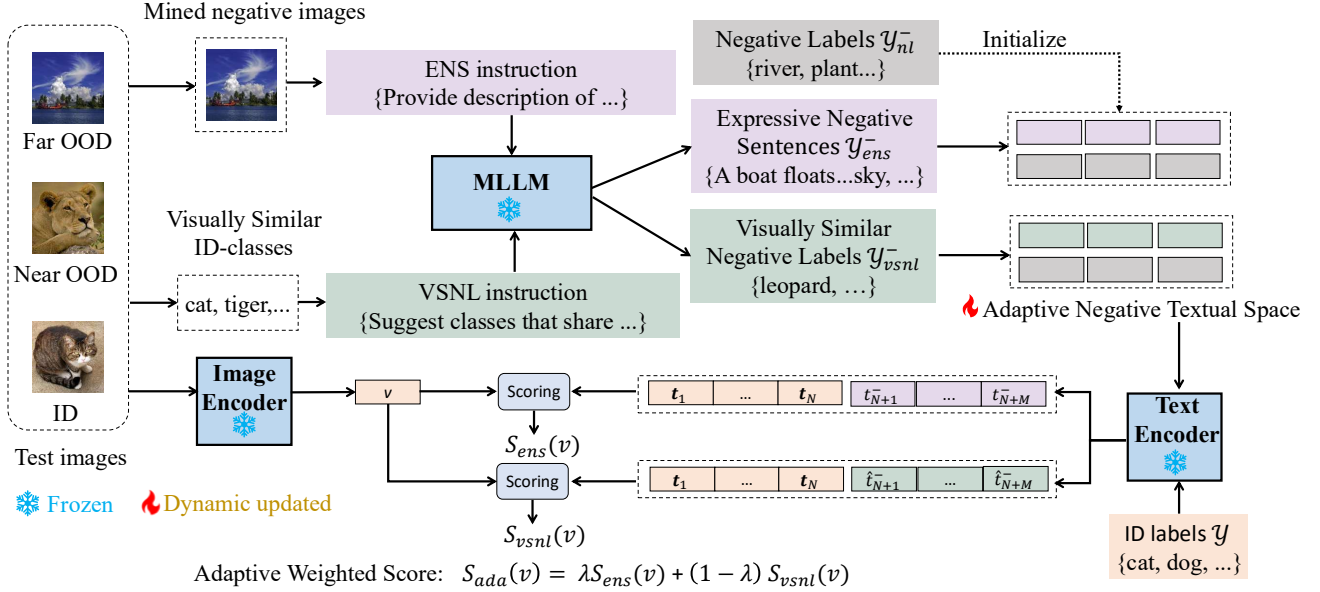


Figure 3. The overall framework of our ANTS. We introduce two negative textual spaces of expressive negative sentences and visually similar negative labels by prompting the MLLM with customized prompts and mined negative images. These two textual spaces are combined with an adaptive weighted score to flexibly handle diverse task settings in open environments.

by analyzing the reconstruction errors within a reconstruction framework. However, traditional methods primarily rely on visual information and often overlook the integration of textual information, limiting their ability to fully leverage multimodal data for OOD detection.

OOD Detection with Vision Language Model. VLM-based OOD detection methods can be broadly categorized into two settings: few-shot and zero-shot. Few-shot methods enhance OOD detection by using negative prompts to define boundaries between ID and OOD images [4, 42, 53], or by integrating non-ID or local ID regions for regularization [35, 51]. For zero-shot OOD detection, some works [33, 48, 77, 84, 88] design post-hoc strategies that utilize softmax scores or image feature information during testing. Some methods [72, 85] leverage auxiliary datasets to strengthen the detection of OOD samples. Other approaches [6, 8, 18, 32, 55] retrieve negative labels from corpus databases or generating them using LLMs. However, these NLs methods lack understanding of actual OOD images, the semantic gap with OOD images limits their OOD detection capabilities.

Multimodal Large Language Models. MLLMs [2, 3, 37, 39, 41, 45] demonstrate strong capabilities across various visual tasks. By integrating large language models, these systems can better interpret instructions and more accurately complete the corresponding tasks. Some approaches [7, 9, 11, 30] have leveraged the understanding and reasoning capabilities of MLLMs for industrial anomaly detection, utilizing their ability to capture fine-grained anomaly semantics. While MLLMs have proven effective in indus-

trial anomaly detection, no prior work has investigated their application to large-scale OOD detection. Our approach is the first to exploit MLLMs’ test time understanding and reasoning capabilities to construct an adaptive and expressive negative textual space, significantly enhancing OOD detection performance.

3. Preliminary

OOD Detection Setup. Denote by \mathcal{X} the image space and $\mathcal{Y} = \{y_1, \dots, y_N\}$ the ID label space, with examples $\mathcal{Y} = \{cat, dog, \dots, bird\}$ and N denoting the total number of classes. Given $x_{in} \in \mathcal{X}$ as the ID random variable and $x_{ood} \in \mathcal{X}$ as the OOD random variable, we denote their respective distributions as $\mathcal{P}_{x_{in}}$ and $\mathcal{P}_{x_{ood}}$. In closed-set scenarios, a test image x is expected to belong to one ID class, i.e., $x \in \mathcal{P}_{x_{in}}$ and $y \in \mathcal{Y}$, where y is the label of x . However, in real-world scenarios, AI systems may encounter samples that do not match any known class, i.e., $x \in \mathcal{P}_{x_{ood}}$ and $y \notin \mathcal{Y}$, resulting in potential misclassifications and safety concerns [52, 61]. To tackle these issues, OOD detection aims to distinguish ID and OOD samples using a scoring function S :

$$G_\gamma(x) = \begin{cases} \text{ID} & S(x) \geq \gamma, \\ \text{OOD} & S(x) < \gamma, \end{cases} \quad (1)$$

where G_γ is the OOD detector with threshold γ .

OOD Detection with NLs. Enhancing OOD detection with textual knowledge has recently garnered increasing attention [48, 72, 84], while a representative type of approach introduces NLs [6, 32]. Specifically, in addition to the ID labels

\mathcal{Y} , these methods introduce a disjoint set of NLs \mathcal{Y}^- and classify a test sample as OOD if it exhibits high similarity to NLs and low similarity to ID labels. In this process, the quality of NLs is crucial. The pioneering method, NegLabel [32], selects words with large cosine distance to ID labels in a large corpus dataset $\mathcal{Y}^c = \{\tilde{y}_1, \tilde{y}_2, \dots, \tilde{y}_K\}$ as NLs:

$$\mathcal{Y}_{nl}^- = \mathcal{G}_{dis}(\mathcal{Y}, \mathcal{Y}^c, f_{clip}, M), \quad (2)$$

where the CLIP-like model f_{clip} defines the label similarity space. K and M represent the numbers of candidate labels in \mathcal{Y}^c and the selected NLs in \mathcal{Y}_{nl}^- , where $M \leq K$. Another representative work, EOE [6], uses prompts to guide an LLM to generate NLs:

$$\mathcal{Y}_{oe}^- = \mathcal{G}_{llm}(\mathcal{Y}, f_{llm}, \rho_{neg}, M), \quad (3)$$

where ρ_{neg} is a carefully designed textual prompt for the LLM f_{llm} . Given the generated NLs (e.g., \mathcal{Y}_{nl}^- [32]), the score function for OOD detection can be formulated as:

$$S_{nl}(\mathbf{v}) = \frac{\sum_{y \in \mathcal{Y}} e^{\cos(\mathbf{v}, \mathbf{t})/\tau}}{\sum_{y \in \mathcal{Y}} e^{\cos(\mathbf{v}, \mathbf{t})/\tau} + \sum_{y^- \in \mathcal{Y}_{nl}^-} e^{\cos(\mathbf{v}, \mathbf{t}^-)/\tau}}, \quad (4)$$

where $\tau > 0$ is the temperature scaling parameter. $\mathbf{v} \in \mathcal{R}^D$ represents the test image feature, while $\mathbf{t} \in \mathcal{R}^D$ and $\mathbf{t}^- \in \mathcal{R}^D$ denote the text features of ID labels $y \in \mathcal{Y}$ and NLs $y^- \in \mathcal{Y}_{nl}^-$, respectively, where D is the feature dimension.

4. Methodology

4.1. Motivation

Although NegLabel [32] and EOE [6] have advanced OOD detection using NLs, they face three key limitations: (1) lacking of understanding of OOD images; (2) poor performance in near-OOD settings due to false negatives by neglecting visually similar classes; and (3) reliance on prior task knowledge, limiting adaptability in open environments. This motivates us to raise the following question: *Can we leverage the test time understanding and reasoning capabilities of MLLMs to shape a more accurate and comprehensive negative textual space?*

In this work, we attempt to answer this question by designing different prompts for MLLMs to shape a more accurate negative textual space, as shown in Fig. 2. The overall pipeline of our method is illustrated in Fig. 3.

4.2. Expressive Negative Sentences

Negative Images Mining. We leverage the image understanding capabilities of MLLMs to generate expressive negative sentences by describing negative images, which are test images likely to be OOD samples. We identify these negative images using the OOD detector of NegLabel, where test images with $S_{nl}(\mathbf{x}) < \gamma$ are selected as negative images:

$$\mathcal{X}_{neg} = \{\mathbf{x} \mid S_{nl}(\mathbf{x}) < \gamma, \mathbf{x} \in \mathcal{X}_{test}\}, \quad (5)$$

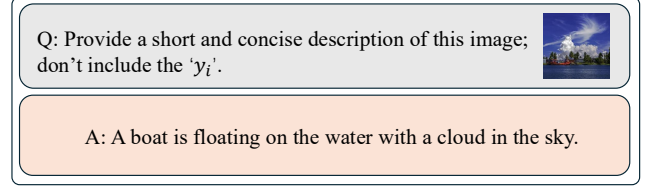


Figure 4. Expressive Negative Sentences, where y_i represents the predicted ID label of the negative image.

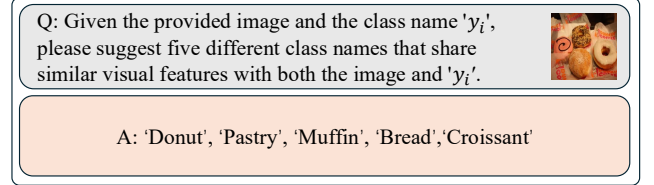


Figure 5. Visually Similar Negative Labels, where y_i represents the predicted ID label of the negative image.

where \mathcal{X}_{test} denotes the test data. We find that manually defining a fixed γ is challenging for handling different testing scenarios, as the optimal threshold varies between near and far OOD settings, as analyzed in Fig. 6b. To address this issue, we develop an adaptive threshold determination strategy based on the characteristics of the test data. Specifically, we first filter out test samples with high S_{nl} scores using Eq. 5, as these samples are highly likely to be ID samples. For the remaining negative images $\hat{\mathcal{X}}_{neg}$, which fall into a mixed set of ID and OOD samples, we select a proportion η of images with the lowest S_{nl} scores, and the adaptive threshold γ^* can be formulated as:

$$\mathcal{X}_{neg} = \text{Top}(\hat{\mathcal{X}}_{neg}, \mathcal{O}_{nl}, \eta), \gamma^* = \arg \max_{\mathbf{x} \in \mathcal{X}_{neg}} S_{nl}(\mathbf{x}), \quad (6)$$

where $\mathcal{O}_{nl} = \{-S_{nl}(\mathbf{x}) \mid \mathbf{x} \in \hat{\mathcal{X}}_{neg}\}$, and $\eta \in (0, 1)$ determines the selection ratio. Here, function $\text{Top}(A, B, \eta)$ selects a proportion of η indices with the highest values in set B , and then retrieves the corresponding images from set A based on these indices. Since this approach relies on the distribution of \mathcal{O}_{nl} , it is equivalent to using an adaptive, data-dependent threshold γ , as illustrated in Fig. 6b.

ENS Generation and Score. With the mined negative images \mathcal{X}_{neg} , we introduce the expressive negative sentences as follows:

$$\mathcal{Y}_{ens}^- = \mathcal{G}_{ens}(\mathcal{Y}, \mathcal{X}_{neg}, f_{mllm}, M), \quad (7)$$

where \mathcal{G}_{ens} is the negative sentence generation process detailed in Fig. 4. If $|\mathcal{X}_{neg}| \geq M$, we randomly select M sentences. Otherwise, we repeat the prompting process to generate M negative sentences. With the expressive negative

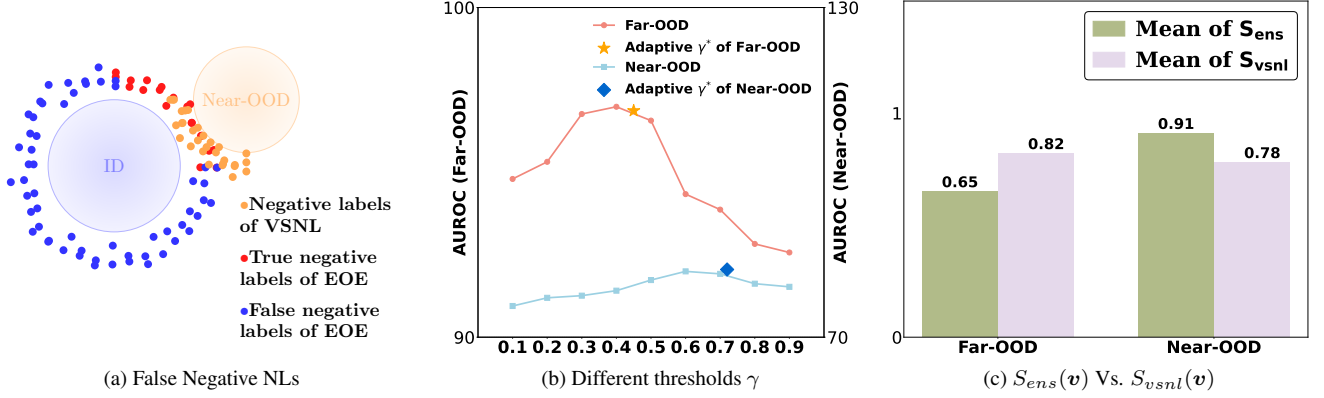


Figure 6. (a) Our VSNL generates visually similar labels only for the ID class subset, whose images are most similar to the near OOD samples, largely reducing false negative labels. (b) Different task settings prefer different thresholds, and our proposed method can adaptively mine negative images, implicitly setting an adaptive threshold. (c) S_{ens} and S_{vsnl} perform differently on far and near OOD, providing clues for designing an adaptive weight λ in Eq. 14.

sentences, we introduce the following negative score:

$$S_{ens}(v) = \frac{\sum_{y \in \mathcal{Y}} e^{\cos(v, t)/\tau}}{\sum_{y \in \mathcal{Y}} e^{\cos(v, t)/\tau} + \sum_{y^- \in \mathcal{Y}_{ens}^-} e^{\cos(v, t^-)/\tau}}. \quad (8)$$

4.3. Visually Similar Negative Labels

The expressive negative sentences introduced above can enhance the detection of far-OOD samples by describing negative images in detail. However, they struggle to distinguish ID samples from visually similar near-OOD data, as both conform to the sentence descriptions. To address this limitation, we prompt the MLLM to generate visually similar labels for the ID labels:

$$\mathcal{Y}_{vsl}^- = \mathcal{G}_{vsnl}(\mathcal{Y}, \mathcal{X}_{neg}, f_{mlm}, M), \quad (9)$$

where \mathcal{G}_{vsnl} represents the visually similar label generation process, as illustrated in Fig. 5.

Visually Similar ID-Classes Mining. While these visually similar labels cover the near-OOD regions, they typically include false NLs. Specifically, OOD data may only be similar to a subset of ID classes, while being distant from others. These visually similar NLs derived from OOD-unrelated ID classes are also far from OOD samples, thereby introducing false NLs and disturbing OOD detection, as intuitively shown in Fig. 6a. To address this issue, we first identify the subset of ID labels most similar to the OOD samples:

$$\mathcal{Y}' = \text{Top}(\mathcal{Y}, F(\mathcal{Y}), \delta), \quad (10)$$

$$F(y_i) = \frac{|\{x \in \mathcal{X}_{neg} \mid H(x) = y_i\}|}{|\mathcal{X}_{neg}|}, \quad \forall y_i \in \mathcal{Y}, \quad (11)$$

where $H(x)$ is the CLIP-based ID classifier with ID text features as weight, $|\cdot|$ measures the set size, $F(y_i)$ represents the proportion of negative images in \mathcal{X}_{neg} being classified

as $y_i \in \mathcal{Y}$, $F(\mathcal{Y})$ is the collection of $F(y_i)$, and $\delta \in (0, 1)$ serves as the selection ratio.

VSNL Generation and Score. After getting these filtered ID labels that share high similarity with negative images, we introduce the following visually similar negative labels:

$$\mathcal{Y}_{vsnl}^- = \mathcal{G}_{vsnl}(\mathcal{Y}', \mathcal{X}_{neg}, f_{mlm}, M). \quad (12)$$

These visually similar negative labels adaptively capture the characteristics of the target OOD distribution, reducing false negative labels and resulting in the following score function:

$$S_{vsnl}(v) = \frac{\sum_{y \in \mathcal{Y}} e^{\cos(v, t)/\tau}}{\sum_{y \in \mathcal{Y}} e^{\cos(v, t)/\tau} + \sum_{y^- \in \mathcal{Y}_{vsnl}^-} e^{\cos(v, \hat{t}^-)/\tau}}, \quad (13)$$

where \hat{t}^- is the text feature of $y^- \in \mathcal{Y}_{vsnl}^-$.

4.4. Adaptive Weighted Score

While expressive negative sentences enhance far-OOD detection by capturing detailed characteristics of negative images, and visually similar negative labels improve near-OOD detection by focusing on OOD-related ID classes, both of them rely on the assumption that the testing scenario (near-OOD or far-OOD) is known beforehand. In real-world applications, this assumption often fails due to the dynamic nature of open environments. To address this, we propose an adaptive weighting strategy to balance these two scoring functions with an adaptive weight $\lambda \in [0, 1]$:

$$S_{ada}(v) = \lambda S_{ens}(v) + (1 - \lambda) S_{vsnl}(v). \quad (14)$$

The weight λ adjusts dynamically based on the environment, approaching 1 in far-OOD scenarios to prioritize $S_{ens}(v)$, and 0 in near-OOD scenarios to emphasize $S_{vsnl}(v)$.

We design the adaptive weight λ by leveraging the performance differences of $S_{ens}(v)$ and $S_{vsnl}(v)$ on near and far

OOD data. Specifically, ENS effectively characterizes far OOD samples, but its coarse-grained descriptions struggle to distinguish near OOD from ID samples, resulting in lower scores for far OOD samples and higher scores for near OOD samples. Conversely, VSNL better captures near OOD samples but, due to its ID-similarity, produces false negatives for far OOD samples, leading to higher scores for far OOD samples and lower scores for near OOD samples, as illustrated in Fig. 6c. Based on this observation, we define λ as:

where $F(a, b) = \frac{1-a}{(1-a)+(1-b)} \in (0, 1)$. One can see that when $\frac{1}{|\mathcal{X}_{neg}|} \sum_{\mathbf{v} \in \mathcal{X}_{neg}^h} S_{ens}(\mathbf{v}) > \frac{1}{|\mathcal{X}_{neg}|} \sum_{\mathbf{v} \in \mathcal{X}_{neg}} S_{vsni}(\mathbf{v})$, λ approaches 0; otherwise, λ approaches 1. The algorithm is summarized in Alg. 1.

5. Experiments

Table 1. OOD detection results by using ImageNet-1k as ID dataset. ViTB/16 is used as the encoder. The results of traditional methods are available in the **supplementary materials**.

Methods	OOD datasets									
	INaturalist		SUN		Places		Textures		Average	
	AUROC↑	FPR95↓	AUROC↑	FPR95↓	AUROC↑	FPR95↓	AUROC↑	FPR95↓	AUROC↑	FPR95↓
Training-required (or with Fine-tuning)										
MSP [22]	87.44	58.36	79.73	73.72	79.67	74.41	79.69	71.93	81.63	69.61
ZOC [18]	86.09	87.30	81.20	81.51	83.39	73.06	76.46	98.90	81.79	85.19
CLIPN [72]	95.27	23.94	93.93	26.17	92.28	33.45	90.93	40.83	93.10	31.10
LSN [53]	95.83	21.56	94.35	26.32	91.25	34.48	90.42	38.54	92.26	30.22
LoCoOp [51]	93.93	29.45	90.32	41.13	90.54	44.15	93.24	33.06	92.01	36.95
ID-Like [4]	98.19	8.98	91.64	42.03	90.57	44.00	94.32	25.27	93.68	30.07
TagOOD [40]	98.97	5.00	92.22	29.70	87.81	40.40	90.60	36.31	92.40	27.85
NegPrompt [42]	90.49	37.79	92.25	32.11	91.16	35.52	88.38	43.93	90.57	37.34
SCT [78]	95.86	13.94	95.33	20.55	92.24	29.86	89.06	41.51	93.27	26.47
CoVer [82]	95.98	22.55	93.42	32.85	90.27	40.71	90.14	43.39	92.45	34.88
LAPT [85]	99.63	1.16	96.01	19.12	92.01	33.01	91.06	40.32	94.68	23.40
CMA [33]	99.62	1.65	96.36	16.84	93.11	27.65	91.64	33.58	95.13	19.93
Zero Shot (No Training Required)										
MCM [48]	94.59	32.20	92.25	38.80	90.31	46.20	86.12	58.50	90.82	43.93
CoVer [82]	95.98	22.55	93.42	32.85	90.27	40.71	90.14	43.39	92.45	34.88
EOE [6]	97.52	12.29	95.73	20.40	92.95	30.16	85.64	57.63	92.96	30.09
NegLabel [32]	99.49	1.91	95.49	20.53	91.64	35.59	90.22	43.56	94.21	25.40
OODD [77]	99.36	2.22	95.01	21.49	87.10	44.76	93.27	30.69	93.69	24.79
CLIPScope [20]	99.61	1.29	96.77	15.56	93.54	28.45	91.41	38.37	95.30	20.88
AdaNeg [84]	99.71	0.59	97.44	9.50	94.55	34.34	94.93	31.27	96.66	18.92
CSP [8]	99.60	1.54	96.66	13.66	92.90	29.32	93.86	25.52	95.76	17.51
ANTS	99.69	0.76	98.53	6.50	95.10	27.45	96.38	18.52	97.40	13.31

Table 2. OOD detection results of zero-shot methods on the OpenOOD benchmark. ImageNet-1k is adopted as ID dataset. Detailed results are available in the **supplementary materials**.

Methods	FPR95 ↓		AUROC ↑	
	Near-OOD	Far-OOD	Near-OOD	Far-OOD
MCM [48]	79.02	68.54	60.11	84.77
NegLabel [32]	68.18	27.34	76.92	93.30
EOE [6]	82.93	46.73	66.94	89.14
AdaNeg [83]	67.51	17.31	76.70	96.43
ANTS	60.98	15.38	82.15	96.50

using ImageNet-10 and ImageNet-20 as ID and OOD data, respectively, and the results are presented in the **supplementary material**, these methods struggle to handle large-scale near-OOD scenarios such as using ImageNet-1k as ID. NegLabel [32] can select negative labels with sufficient semantic differences from ID labels, but it cannot effectively represent near-OOD semantics. EOE [6] uses LLM to generate visually similar labels for all ID classes, bringing a large amount of false negative labels with the increase in the number of ID classes. Our proposed ANTS first identifies a subset of ID classes similar to OOD images, as shown in

Table 3. Ablation experiments. ‘NIM’ indicates the Negative Image Mining strategy in Eq. 6, and ‘SIM’ means the Visually Similar ID-Classes Mining strategy in Eq. 10.

	Components					FPR95 ↓	
	NIM	\mathcal{Y}_{ens}^-	SIM	\mathcal{Y}_{vsnl}^-	$S_{ada}(\mathbf{v})$	NearOOD	FarOOD
NegLabel[32]						68.18	27.34
A	✗	✓	✗	✗	✗	74.48	43.87
B	✓	✓	✗	✗	✗	73.70	19.22
C	✗	✗	✗	✓	✗	74.36	53.82
D	✗	✗	✓	✓	✗	63.11	23.44
E	✓	✓	✓	✓	✗	62.05	21.65
F	✓	✓	✓	✓	✓	60.98	15.38

Fig. 6a, then leverages the reasoning capabilities of MLLMs to generate visually similar labels. As a result, ANTS significantly outperforms its closest competitors [6, 32, 84] in both near-OOD and far-OOD scenarios, validating its scalability.

5.3. Analyses and Discussions

Ablation Study. As illustrated in Tab. 3, it is necessary to introduce ENS \mathcal{Y}_{ens}^- with mined negative images, as validated by the advantages of setting B over A in the far-OOD setting. Setting B significantly outperforms NegLabel, confirming

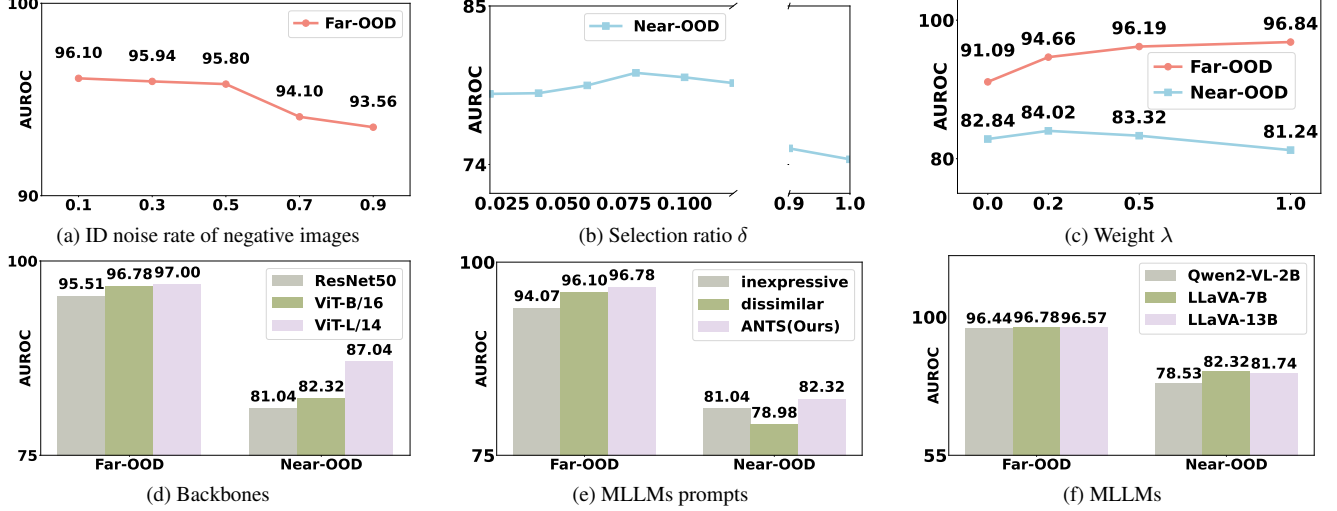


Figure 7. Analysis on (a) length of negative text, (b) selection ratio δ , (c) weight λ , (d) CLIP image encoder backbones, (e) MLLMs prompts, and (f) different MLLMs. We use Texture [10] and NINCO [5] datasets as Far-OOD and Near-OOD, respectively.

the superiority of ENS over NLS. Generating visually similar labels to the mined ID class subset can significantly reduce false negative labels, as justified by the advantages of setting D over C. Combining ENS with VSNL by setting $\lambda = 0.5$ balances the results across different OOD sets, as shown in setting E, while using an adaptive λ leads to the best results in both OOD scenarios, as shown in setting F.

Robustness of ANTS to Noisy Negative Images. We investigate the impact of different rates of ID noise in negative images on the model OOD detection performance, as shown in Fig. 7a. When the ID ratio of negative images is relatively low (less than 0.5), our ANTS achieves excellent OOD detection performance across different ID ratios. This demonstrates the robustness of ANTS against ID noise.

Ratio δ . As shown in Fig. 7b, generating visually similar labels for all ID classes ($\delta = 1$) performs poorly due to numerous false negative labels, as illustrated in Fig. 6a. However, using a too small δ will fail to adequately cover the OOD distribution. We set $\delta = 0.08$ in all experiments, although it is not optimal for specific datasets.

Weight λ . As shown in Fig. 7c, a larger λ emphasizes the $S_{ens}(x)$ score, improving far-OOD detection, while a smaller λ prioritizes the $S_{vsnl}(x)$ score, enhancing near-OOD detection. Our adaptive strategy automatically selects a suitable λ for various OOD settings.

Different Backbones. As illustrated in Fig. 7d, larger visual backbones generally achieve improved OOD detection. Besides, our ANTS can generalize well to various VLM backbones, demonstrating its robustness.

Different Prompts for MLLMs. To investigate the effectiveness of the prompts for ENS and VSNL, we designed two additional prompts: an inexpressive prompt and a dissimilar prompt. Specifically, the inexpressive prompt asks MLLMs to generate descriptions for negative images using less than

Table 4. Complexity analyses. All results are obtained by using a GeForce RTX 3090 GPU.

Methods	Training Time	Images per Second	Param.
ZOC	> 24 h	186	336 M
CLIPN	> 24 h	396	37.8 M
EOE	-	392	-
NegLabel	-	384	-
AdaNeg	-	370	-
ANTS	-	356	-

three words. The dissimilar prompt prompts MLLMs to generate negative categories that are visually dissimilar to the high frequency ID classes. As shown in Fig. 7e, OOD detection performance degrades with these two instructions, demonstrating the effectiveness of our proposed prompts.

Various MLLMs. To investigate the impact of different MLLMs in adaptive negative textual space construction, we conducted experiments using MLLMs with varying parameter sizes, as illustrated in Fig. 7f. Models of different sizes show little variation in performance on far OOD. However, in the near-OOD settings, larger MLLMs perform better due to their stronger reasoning capabilities and LLaVA-7B achieves the best performance.

Complexity Analyses. As analyzed in Tab. 4, our ANTS requires no model training or learnable parameters. By using a small MLLM and decreasing the number of negative images, ANTS mitigates the impact of slow inference caused by MLLMs, maintaining a fast inference speed.

More Analyses. Analyses of Robustness to Domain Shift, Instantiations of Adaptive Weighted Score and Temporal Shift are available in the **supplementary materials**.

6. Conclusion and Limitation

This paper presented a novel adaptive negative textual space by leveraging the understanding and reasoning capabilities of MLLMs. We first identified three limitations of existing NLS-based methods: a lack of understanding of OOD images, difficulty addressing the challenging near-OOD setting, and reliance on the strong assumption of the target task setting. Then, we designed two types of prompts to leverage the test time understanding and reasoning capabilities of MLLMs to generate expressive negative sentences and visually similar labels. To avoid interference from ID noise and generate false negative labels, we designed two strategies: Negative Images Mining and Visually Similar ID Classes Mining. Finally, an adaptive weight was designed to balance these two text spaces in open environments. Experiments demonstrated the significant advantages of our ANTS over other zero-shot OOD detection methods.

Despite the advantages, there are some limitations of ANTS. First, it relies on a basic OOD detector to select negative images in the first stage. Although ANTS is robust to ID noise, it still requires a large number of negative images to ensure the extensive negative space. Additionally, leveraging the understanding and reasoning capabilities of MLLMs during test time incurs extra cost, which motivates us to explore a more efficient use of MLLMs in the future.

References

- [1] Davide Abati, Angelo Porrello, Simone Calderara, and Rita Cucchiara. Latent space autoregression for novelty detection. In *Proceedings of the IEEE/CVF conference on computer vision and pattern recognition*, pages 481–490, 2019.
- [2] Josh Achiam, Steven Adler, Sandhini Agarwal, Lama Ahmad, Ilge Akkaya, Florencia Leoni Aleman, Diogo Almeida, Janko Altmenschmidt, Sam Altman, Shyamal Anadkat, et al. Gpt-4 technical report. *arXiv preprint arXiv:2303.08774*, 2023.
- [3] Shuai Bai, Keqin Chen, Xuejing Liu, Jialin Wang, Wenbin Ge, Sibao Song, Kai Dang, Peng Wang, Shijie Wang, Jun Tang, et al. Qwen2. 5-vl technical report. *arXiv preprint arXiv:2502.13923*, 2025.
- [4] Yichen Bai, Zongbo Han, Bing Cao, Xiaoheng Jiang, Qinghua Hu, and Changqing Zhang. Id-like prompt learning for few-shot out-of-distribution detection. In *Proceedings of the IEEE/CVF Conference on Computer Vision and Pattern Recognition*, pages 17480–17489, 2024.
- [5] Julian Bitterwolf, Maximilian Mueller, and Matthias Hein. In or out? fixing imagenet out-of-distribution detection evaluation. *arXiv preprint arXiv:2306.00826*, 2023.
- [6] Chentao Cao, Zhun Zhong, Zhanke Zhou, Yang Liu, Tongliang Liu, and Bo Han. Envisioning outlier exposure by large language models for out-of-distribution detection. *arXiv preprint arXiv:2406.00806*, 2024.
- [7] Yuhao Chao, Jie Liu, Jie Tang, and Gangshan Wu. Anomaly1: A gpo-based end-to-end mllm for industrial anomaly detection. *arXiv preprint arXiv:2504.11914*, 2025.
- [8] Mengyuan Chen, Junyu Gao, and Changsheng Xu. Conjugated semantic pool improves ood detection with pre-trained vision-language models. *arXiv preprint arXiv:2410.08611*, 2024.
- [9] Zhiling Chen, Hanning Chen, Mohsen Imani, and Farhad Imani. Can multimodal large language models be guided to improve industrial anomaly detection? *arXiv preprint arXiv:2501.15795*, 2025.
- [10] Mircea Cimpoi, Subhransu Maji, Iasonas Kokkinos, Sammy Mohamed, and Andrea Vedaldi. Describing textures in the wild. In *Proceedings of the IEEE conference on computer vision and pattern recognition*, pages 3606–3613, 2014.
- [11] Huilin Deng, Hongchen Luo, Wei Zhai, Yang Cao, and Yu Kang. Vmad: Visual-enhanced multimodal large language model for zero-shot anomaly detection. *arXiv preprint arXiv:2409.20146*, 2024.
- [12] Jia Deng, Wei Dong, Richard Socher, Li-Jia Li, Kai Li, and Li Fei-Fei. Imagenet: A large-scale hierarchical image database. In *2009 IEEE conference on computer vision and pattern recognition*, pages 248–255. Ieee, 2009.
- [13] Taylor Denouden, Rick Salay, Krzysztof Czarnecki, Vahdat Abdelzad, Buu Phan, and Sachin Vernekar. Improving reconstruction autoencoder out-of-distribution detection with mahalanobis distance. *arXiv preprint arXiv:1812.02765*, 2018.
- [14] Andrija Djuricic, Nebojsa Bozanic, Arjun Ashok, and Rosanne Liu. Extremely simple activation shaping for out-of-distribution detection. *arXiv preprint arXiv:2209.09858*, 2022.
- [15] Xin Dong, Junfeng Guo, Ang Li, Wei-Te Ting, Cong Liu, and HT Kung. Neural mean discrepancy for efficient out-of-distribution detection. In *Proceedings of the IEEE/CVF Conference on Computer Vision and Pattern Recognition*, pages 19217–19227, 2022.
- [16] Alexey Dosovitskiy, Lucas Beyer, Alexander Kolesnikov, Dirk Weissenborn, Xiaohua Zhai, Thomas Unterthiner, Mostafa Dehghani, Matthias Minderer, Georg Heigold, Sylvain Gelly, et al. An image is worth 16x16 words: Transformers for image recognition at scale. *arXiv preprint arXiv:2010.11929*, 2020.
- [17] Xuefeng Du, Xin Wang, Gabriel Gozum, and Yixuan Li. Unknown-aware object detection: Learning what you don’t know from videos in the wild. In *Proceedings of the IEEE/CVF Conference on Computer Vision and Pattern Recognition*, pages 13678–13688, 2022.
- [18] Sepideh Esmailpour, Bing Liu, Eric Robertson, and Lei Shu. Zero-shot out-of-distribution detection based on the pre-trained model clip. In *Proceedings of the AAAI conference on artificial intelligence*, pages 6568–6576, 2022.
- [19] Stanislav Fort, Jie Ren, and Balaji Lakshminarayanan. Exploring the limits of out-of-distribution detection. *Advances in Neural Information Processing Systems*, 34:7068–7081, 2021.
- [20] Hao Fu, Naman Patel, Prashanth Krishnamurthy, and Farshad Khorrami. Clipse: Enhancing zero-shot ood detection with bayesian scoring. In *2025 IEEE/CVF Winter Conference on Applications of Computer Vision (WACV)*, pages 5346–5355. IEEE, 2025.

- [21] Kaiming He, Xiangyu Zhang, Shaoqing Ren, and Jian Sun. Deep residual learning for image recognition. In *Proceedings of the IEEE conference on computer vision and pattern recognition*, pages 770–778, 2016.
- [22] Dan Hendrycks and Kevin Gimpel. A baseline for detecting misclassified and out-of-distribution examples in neural networks. *arXiv preprint arXiv:1610.02136*, 2016.
- [23] Dan Hendrycks, Mantas Mazeika, and Thomas Dietterich. Deep anomaly detection with outlier exposure. *arXiv preprint arXiv:1812.04606*, 2018.
- [24] Dan Hendrycks, Norman Mu, Ekin D Cubuk, Barret Zoph, Justin Gilmer, and Balaji Lakshminarayanan. Augmix: A simple data processing method to improve robustness and uncertainty. *arXiv preprint arXiv:1912.02781*, 2019.
- [25] Yen-Chang Hsu, Yilin Shen, Hongxia Jin, and Zsolt Kira. Generalized odin: Detecting out-of-distribution image without learning from out-of-distribution data. In *Proceedings of the IEEE/CVF conference on computer vision and pattern recognition*, pages 10951–10960, 2020.
- [26] Rui Huang and Yixuan Li. Mos: Towards scaling out-of-distribution detection for large semantic space. In *Proceedings of the IEEE/CVF Conference on Computer Vision and Pattern Recognition*, pages 8710–8719, 2021.
- [27] Rui Huang, Andrew Geng, and Yixuan Li. On the importance of gradients for detecting distributional shifts in the wild. *Advances in Neural Information Processing Systems*, 34:677–689, 2021.
- [28] Dihong Jiang, Sun Sun, and Yaoliang Yu. Revisiting flow generative models for out-of-distribution detection. In *International Conference on Learning Representations*, 2021.
- [29] Wenyu Jiang, Yuxin Ge, Hao Cheng, Mingcai Chen, Shuai Feng, and Chongjun Wang. Read: Aggregating reconstruction error into out-of-distribution detection. In *Proceedings of the AAAI Conference on Artificial Intelligence*, pages 14910–14918, 2023.
- [30] Xi Jiang, Jian Li, Hanqiu Deng, Yong Liu, Bin-Bin Gao, Yifeng Zhou, Jialin Li, Chengjie Wang, and Feng Zheng. Mmad: A comprehensive benchmark for multimodal large language models in industrial anomaly detection. In *The Thirteenth International Conference on Learning Representations*.
- [31] Xue Jiang, Feng Liu, Zhen Fang, Hong Chen, Tongliang Liu, Feng Zheng, and Bo Han. Detecting out-of-distribution data through in-distribution class prior. In *International Conference on Machine Learning*, pages 15067–15088. PMLR, 2023.
- [32] Xue Jiang, Feng Liu, Zhen Fang, Hong Chen, Tongliang Liu, Feng Zheng, and Bo Han. Negative label guided ood detection with pretrained vision-language models. *arXiv preprint arXiv:2403.20078*, 2024.
- [33] Jeonghyeon Kim and Sangheum Hwang. Enhanced ood detection through cross-modal alignment of multi-modal representations. In *Proceedings of the Computer Vision and Pattern Recognition Conference*, pages 29979–29988, 2025.
- [34] Alex Krizhevsky, Geoffrey Hinton, et al. Learning multiple layers of features from tiny images. 2009.
- [35] Marc Lafon, Elias Ramzi, Clément Rambour, Nicolas Audebert, and Nicolas Thome. Gallop: Learning global and local prompts for vision-language models. In *European Conference on Computer Vision*, pages 264–282. Springer, 2024.
- [36] Kimin Lee, Kibok Lee, Honglak Lee, and Jinwoo Shin. A simple unified framework for detecting out-of-distribution samples and adversarial attacks. *Advances in neural information processing systems*, 31, 2018.
- [37] Boyi Li, Kilian Q Weinberger, Serge Belongie, Vladlen Koltun, and René Ranftl. Language-driven semantic segmentation. *arXiv preprint arXiv:2201.03546*, 2022.
- [38] Jingyao Li, Pengguang Chen, Zexin He, Shaozuo Yu, Shu Liu, and Jiaya Jia. Rethinking out-of-distribution (ood) detection: Masked image modeling is all you need. In *Proceedings of the IEEE/CVF conference on computer vision and pattern recognition*, pages 11578–11589, 2023.
- [39] Junnan Li, Dongxu Li, Silvio Savarese, and Steven Hoi. Blip-2: Bootstrapping language-image pre-training with frozen image encoders and large language models. In *International conference on machine learning*, pages 19730–19742. PMLR, 2023.
- [40] Jinglun Li, Xinyu Zhou, Kaixun Jiang, Lingyi Hong, Pinxue Guo, Zhaoyu Chen, Weifeng Ge, and Wenqiang Zhang. Tagood: A novel approach to out-of-distribution detection via vision-language representations and class center learning. In *Proceedings of the 32nd ACM International Conference on Multimedia*, pages 1225–1234, 2024.
- [41] Liunian Harold Li, Pengchuan Zhang, Haotian Zhang, Jianwei Yang, Chunyuan Li, Yiwu Zhong, Lijuan Wang, Lu Yuan, Lei Zhang, Jenq-Neng Hwang, et al. Grounded language-image pre-training. In *Proceedings of the IEEE/CVF conference on computer vision and pattern recognition*, pages 10965–10975, 2022.
- [42] Tianqi Li, Guansong Pang, Xiao Bai, Wenjun Miao, and Jin Zheng. Learning transferable negative prompts for out-of-distribution detection. In *Proceedings of the IEEE/CVF Conference on Computer Vision and Pattern Recognition*, pages 17584–17594, 2024.
- [43] Shiyu Liang, Yixuan Li, and Rayadurgam Srikant. Enhancing the reliability of out-of-distribution image detection in neural networks. *arXiv preprint arXiv:1706.02690*, 2017.
- [44] Ziqian Lin, Sreya Dutta Roy, and Yixuan Li. Mood: Multi-level out-of-distribution detection. In *Proceedings of the IEEE/CVF conference on Computer Vision and Pattern Recognition*, pages 15313–15323, 2021.
- [45] Haotian Liu, Chunyuan Li, Qingyang Wu, and Yong Jae Lee. Visual instruction tuning. *Advances in neural information processing systems*, 36:34892–34916, 2023.
- [46] Weitang Liu, Xiaoyun Wang, John Owens, and Yixuan Li. Energy-based out-of-distribution detection. *Advances in neural information processing systems*, 33:21464–21475, 2020.
- [47] Xixi Liu, Yaroslava Lochman, and Christopher Zach. Gen: Pushing the limits of softmax-based out-of-distribution detection. In *Proceedings of the IEEE/CVF conference on computer vision and pattern recognition*, pages 23946–23955, 2023.
- [48] Yifei Ming, Ziyang Cai, Jiuxiang Gu, Yiyun Sun, Wei Li, and Yixuan Li. Delving into out-of-distribution detection with vision-language representations. *Advances in neural information processing systems*, 35:35087–35102, 2022.

- [49] Yifei Ming, Ying Fan, and Yixuan Li. Poem: Out-of-distribution detection with posterior sampling. In *International Conference on Machine Learning*, pages 15650–15665. PMLR, 2022.
- [50] Yifei Ming, Yiyoun Sun, Ousmane Dia, and Yixuan Li. How to exploit hyperspherical embeddings for out-of-distribution detection? *arXiv preprint arXiv:2203.04450*, 2022.
- [51] Atsuyuki Miyai, Qing Yu, Go Irie, and Kiyoharu Aizawa. Locoop: Few-shot out-of-distribution detection via prompt learning. *Advances in Neural Information Processing Systems*, 36, 2024.
- [52] Anh Nguyen, Jason Yosinski, and Jeff Clune. Deep neural networks are easily fooled: High confidence predictions for unrecognizable images. In *Proceedings of the IEEE conference on computer vision and pattern recognition*, pages 427–436, 2015.
- [53] Jun Nie, Yonggang Zhang, Zhen Fang, Tongliang Liu, Bo Han, and Xinmei Tian. Out-of-distribution detection with negative prompts. In *The Twelfth International Conference on Learning Representations*, 2024.
- [54] Aristotelis-Angelos Papadopoulos, Mohammad Reza Rajati, Nazim Shaikh, and Jiamian Wang. Outlier exposure with confidence control for out-of-distribution detection. *Neurocomputing*, 441:138–150, 2021.
- [55] Jaewoo Park, Yoon Gyo Jung, and Andrew Beng Jin Teoh. Nearest neighbor guidance for out-of-distribution detection. In *Proceedings of the IEEE/CVF International Conference on Computer Vision*, pages 1686–1695, 2023.
- [56] Stanislav Pidhorskyi, Ranya Almohsen, and Gianfranco Doretto. Generative probabilistic novelty detection with adversarial autoencoders. *Advances in neural information processing systems*, 31, 2018.
- [57] Alec Radford, Jong Wook Kim, Chris Hallacy, Aditya Ramesh, Gabriel Goh, Sandhini Agarwal, Girish Sastry, Amanda Askell, Pamela Mishkin, Jack Clark, et al. Learning transferable visual models from natural language supervision. In *International conference on machine learning*, pages 8748–8763. PMLR, 2021.
- [58] Jie Ren, Peter J Liu, Emily Fertig, Jasper Snoek, Ryan Poplin, Mark Depristo, Joshua Dillon, and Balaji Lakshminarayanan. Likelihood ratios for out-of-distribution detection. *Advances in neural information processing systems*, 32, 2019.
- [59] Jie Ren, Stanislav Fort, Jeremiah Liu, Abhijit Guha Roy, Shreyas Padhy, and Balaji Lakshminarayanan. A simple fix to mahalanobis distance for improving near-ood detection. *arXiv preprint arXiv:2106.09022*, 2021.
- [60] Chandramouli Shama Sastry and Sageev Oore. Detecting out-of-distribution examples with gram matrices. In *International Conference on Machine Learning*, pages 8491–8501. PMLR, 2020.
- [61] Walter J Scheirer, Anderson de Rezende Rocha, Archana Sapkota, and Terrance E Boult. Toward open set recognition. *IEEE transactions on pattern analysis and machine intelligence*, 35(7):1757–1772, 2012.
- [62] Yiyoun Sun and Yixuan Li. Dice: Leveraging sparsification for out-of-distribution detection. In *European Conference on Computer Vision*, pages 691–708. Springer, 2022.
- [63] Yiyoun Sun, Chuan Guo, and Yixuan Li. React: Out-of-distribution detection with rectified activations. *Advances in Neural Information Processing Systems*, 34:144–157, 2021.
- [64] Yiyoun Sun, Yifei Ming, Xiaojin Zhu, and Yixuan Li. Out-of-distribution detection with deep nearest neighbors. In *International Conference on Machine Learning*, pages 20827–20840. PMLR, 2022.
- [65] Leitian Tao, Xuefeng Du, Xiaojin Zhu, and Yixuan Li. Non-parametric outlier synthesis. *arXiv preprint arXiv:2303.02966*, 2023.
- [66] Sunil Thulasidasan, Gopinath Chennupati, Jeff A Bilmes, Tammo Bhattacharya, and Sarah Michalak. On mixup training: Improved calibration and predictive uncertainty for deep neural networks. *Advances in neural information processing systems*, 32, 2019.
- [67] Joost Van Amersfoort, Lewis Smith, Yee Whye Teh, and Yarin Gal. Uncertainty estimation using a single deep deterministic neural network. In *International conference on machine learning*, pages 9690–9700. PMLR, 2020.
- [68] Grant Van Horn, Oisin Mac Aodha, Yang Song, Yin Cui, Chen Sun, Alex Shepard, Hartwig Adam, Pietro Perona, and Serge Belongie. The inaturalist species classification and detection dataset. In *Proceedings of the IEEE conference on computer vision and pattern recognition*, pages 8769–8778, 2018.
- [69] Sagar Vaze, Kai Han, Andrea Vedaldi, and Andrew Zisserman. Open-set recognition: A good closed-set classifier is all you need? 2021.
- [70] Haoran Wang, Weitang Liu, Alex Bocchieri, and Yixuan Li. Can multi-label classification networks know what they don’t know? *Advances in Neural Information Processing Systems*, 34:29074–29087, 2021.
- [71] Haoqi Wang, Zhizhong Li, Litong Feng, and Wayne Zhang. Vim: Out-of-distribution with virtual-logit matching. In *Proceedings of the IEEE/CVF conference on computer vision and pattern recognition*, pages 4921–4930, 2022.
- [72] Hualiang Wang, Yi Li, Huifeng Yao, and Xiaomeng Li. Clipn for zero-shot ood detection: Teaching clip to say no. In *Proceedings of the IEEE/CVF International Conference on Computer Vision*, pages 1802–1812, 2023.
- [73] Yezhen Wang, Bo Li, Tong Che, Kaiyang Zhou, Ziwei Liu, and Dongsheng Li. Energy-based open-world uncertainty modeling for confidence calibration. In *Proceedings of the IEEE/CVF International Conference on Computer Vision*, pages 9302–9311, 2021.
- [74] Hongxin Wei, Renchunzi Xie, Hao Cheng, Lei Feng, Bo An, and Yixuan Li. Mitigating neural network overconfidence with logit normalization. In *International conference on machine learning*, pages 23631–23644. PMLR, 2022.
- [75] Jianxiong Xiao, James Hays, Krista A Ehinger, Aude Oliva, and Antonio Torralba. Sun database: Large-scale scene recognition from abbey to zoo. In *2010 IEEE computer society conference on computer vision and pattern recognition*, pages 3485–3492. IEEE, 2010.
- [76] Yijun Yang, Ruiyuan Gao, and Qiang Xu. Out-of-distribution detection with semantic mismatch under masking. In *European Conference on Computer Vision*, pages 373–390. Springer, 2022.

- [77] Yifeng Yang, Lin Zhu, Zewen Sun, Hengyu Liu, Qinying Gu, and Nanyang Ye. Odd: Test-time out-of-distribution detection with dynamic dictionary. *arXiv preprint arXiv:2503.10468*, 2025.
- [78] Geng Yu, Jianing Zhu, Jiangchao Yao, and Bo Han. Self-calibrated tuning of vision-language models for out-of-distribution detection. *Advances in Neural Information Processing Systems*, 37:56322–56348, 2024.
- [79] Qing Yu and Kiyoharu Aizawa. Unsupervised out-of-distribution detection by maximum classifier discrepancy. In *Proceedings of the IEEE/CVF international conference on computer vision*, pages 9518–9526, 2019.
- [80] Sangdoo Yun, Dongyoon Han, Seong Joon Oh, Sanghyuk Chun, Junsuk Choe, and Youngjoon Yoo. Cutmix: Regularization strategy to train strong classifiers with localizable features. In *Proceedings of the IEEE/CVF international conference on computer vision*, pages 6023–6032, 2019.
- [81] Alireza Zaeemzadeh, Niccolo Bisagno, Zeno Sambugaro, Nicola Conci, Nazanin Rahnavard, and Mubarak Shah. Out-of-distribution detection using union of 1-dimensional subspaces. In *Proceedings of the IEEE/CVF conference on Computer Vision and Pattern Recognition*, pages 9452–9461, 2021.
- [82] Boxuan Zhang, Jianing Zhu, Zengmao Wang, Tongliang Liu, Bo Du, and Bo Han. What if the input is expanded in ood detection? *Advances in Neural Information Processing Systems*, 37:21289–21329, 2024.
- [83] Jinsong Zhang, Qiang Fu, Xu Chen, Lun Du, Zelin Li, Gang Wang, Shi Han, Dongmei Zhang, et al. Out-of-distribution detection based on in-distribution data patterns memorization with modern hopfield energy. In *The Eleventh International Conference on Learning Representations*, 2022.
- [84] Yabin Zhang and Lei Zhang. Adaneg: Adaptive negative proxy guided ood detection with vision-language models. *arXiv preprint arXiv:2410.20149*, 2024.
- [85] Yabin Zhang, Wenjie Zhu, Chenhang He, and Lei Zhang. Lapt: Label-driven automated prompt tuning for ood detection with vision-language models. *arXiv preprint arXiv:2407.08966*, 2024.
- [86] Bolei Zhou, Agata Lapedriza, Aditya Khosla, Aude Oliva, and Antonio Torralba. Places: A 10 million image database for scene recognition. *IEEE transactions on pattern analysis and machine intelligence*, 40(6):1452–1464, 2017.
- [87] Yibo Zhou. Rethinking reconstruction autoencoder-based out-of-distribution detection. In *Proceedings of the IEEE/CVF Conference on Computer Vision and Pattern Recognition*, pages 7379–7387, 2022.
- [88] Wenjie Zhu, Yabin Zhang, Xin Jin, Wenjun Zeng, and Lei Zhang. Knowledge regularized negative feature tuning for out-of-distribution detection with vision-language models. *arXiv preprint arXiv:2507.19847*, 2025.
- [89] Bo Zong, Qi Song, Martin Renqiang Min, Wei Cheng, Cristian Lumezanu, Daeki Cho, and Haifeng Chen. Deep autoencoding gaussian mixture model for unsupervised anomaly detection. In *International conference on learning representations*, 2018.

Supplementary Materials

A. More Results

Full Comparison on ImageNet Benchmark. Full comparisons with more competitors on the ImageNet benchmark are illustrated in Tab. 5, including the results of traditional methods [17, 22, 27, 43, 46, 64, 71] by fine-tuning CLIP visual encoder with labeled training samples following [32]. Compared with other traditional OOD detection methods that require fine-tuning, our ANTS is training-free and achieves better OOD detection performance on ImageNet-1k.

Results on OpenOOD Benchmark. The OpenOOD benchmark results are presented in Tab. 6, including the results of other methods requiring manually labeled training samples. Compared with other methods [24, 47, 59] that require manually labeled training samples, our ANTS model operates in a zero-shot manner and does not require training. Furthermore, our ANTS surpasses other CLIP-based zero-shot OOD detection methods on both far-OOD and near-OOD tasks in the OpenOOD benchmark.

Detailed OOD Detection Results of ANTS on OpenOOD Benchmark. The detailed OOD detection results of ANTS on the OpenOOD benchmark are shown in Tab. 7. We see that ANTS achieves good results in both Far-OOD and Near-OOD scenarios, demonstrating its strong adaptability to different OOD situations.

Temporal Shift. In real-world scenarios, there are often a large number of near-ood and far-ood samples that occur simultaneously, and we cannot determine their order of occurrence in advance. To explore the impact of temporal shift caused by their order of appearance on OOD detection results, we conducted experiments by using different temporal shifts. As illustrated in Fig. 8, ANTS achieves good results under different temporal shifts, demonstrating its robustness to temporal shift.

Near-OOD Detection. We alternate the use of ImageNet-10 and ImageNet-20 as ID and OOD datasets. The results are shown in Tab. 8. We see that ANTS significantly outperforms EOE and AdaNeg under the two experimental settings, demonstrating the advantage of our constructed adaptive negative text space.

Other Instantiations of Adaptive Weighted Score. As shown in Tab. 9, we consider various instantiations of the adaptive weighted score function. Specifically, we examine functions that employ only the ENS score, only the VSNL score, as well as logarithmic, exponential, and fractional functions. The results indicate that using the fractional function in conjunction with the ENS score and VSNL score yields the best results.

Robustness to Domain Shift. To verify the robustness of ANTS to domain shift, we test several variants of ImageNet with different domain shifts. As shown in Tab. 10,

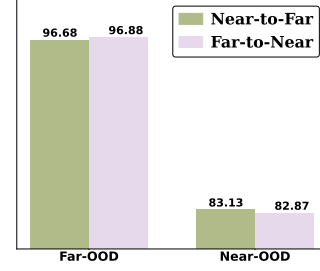


Figure 8. Analysis of Temporal Shift, where ImageNet1k is adopted as the ID dataset, NINCO and Texture are adopted as the Near-OOD and Far-OOD, respectively. ‘Near-to-Far’ indicates that testing begins with Near-OOD samples and continues with Far-OOD samples using the ENS and VSNL initialized from Near-OOD. ‘Far-to-Near’ is the opposite process.

ANTS outperforms MCM and NegLabels on the four different ID datasets, highlighting the remarkable robustness of our ANTS to domain shifts.

Zero-shot OOD Detection Results with Various ID Datasets. We compare the zero-shot OOD detection performance of ANTS and other methods on several ID datasets. As illustrated in Tab. 11, ANTS outperforms the other three methods across different ID datasets.

B. Case Study

To better illustrate the effectiveness of ANTS, we visualize the adaptive negative text space with some ID and OOD images for a case study, as shown in Fig. 9. We see that images from the ID dataset exhibit high similarity to the ID classes. For Far-OOD, as shown in Fig. 10, the images from the OOD dataset demonstrate high similarity to the ENS space. For Near-OOD, as shown in Fig. 11, the images from the OOD dataset show a high similarity to the VSNL space.

Table 5. OOD detection results by using ImageNet-1k as the ID dataset. ViTB/16 is used as the encoder.

Methods	OOD datasets									
	INaturalist		SUN		Places		Textures		Average	
	AUROC↑	FPR95↓	AUROC↑	FPR95↓	AUROC↑	FPR95↓	AUROC↑	FPR95↓	AUROC↑	FPR95↓
Training-required (or with Fine-tuning)										
MSP [22]	87.44	58.36	79.73	73.72	79.67	74.41	79.69	71.93	81.63	69.61
ODIN [43]	94.65	30.22	87.17	54.04	85.54	55.06	87.85	51.67	88.80	47.75
Energy [46]	95.33	26.12	92.66	35.97	91.41	39.87	86.76	57.61	91.54	39.89
GradNorm [27]	72.56	81.50	72.86	82.00	73.70	80.41	70.26	79.36	72.35	80.82
ViM [71]	93.16	32.19	87.19	54.01	83.75	60.67	87.18	53.94	87.82	50.20
KNN [64]	94.52	29.17	92.67	35.62	91.02	39.61	85.67	64.35	90.97	42.19
VOS [17]	94.62	28.99	92.57	36.88	91.23	38.39	86.33	61.02	91.19	41.32
NPOS [65]	96.19	16.58	90.44	43.77	89.44	45.27	88.80	46.12	91.22	37.93
ZOC [18]	86.09	87.30	81.20	81.51	83.39	73.06	76.46	98.90	81.79	85.19
CLIPN [72]	95.27	23.94	93.93	26.17	92.28	33.45	90.93	40.83	93.10	31.10
LSN [53]	95.83	21.56	94.35	26.32	91.25	34.48	90.42	38.54	92.26	30.22
LoCoOp [51]	93.93	29.45	90.32	41.13	90.54	44.15	93.24	33.06	92.01	36.95
ID-Like [4]	98.19	8.98	91.64	42.03	90.57	44.00	94.32	25.27	93.68	30.07
NegPrompt [42]	90.49	37.79	92.25	32.11	91.16	35.52	88.38	43.93	90.57	37.34
CoVer [82]	95.98	22.55	93.42	32.85	90.27	40.71	90.14	43.39	92.45	34.88
SCT [42]	95.86	13.94	95.33	20.55	92.24	29.86	89.06	41.51	93.27	26.47
LAPT [85]	99.63	1.16	96.01	19.12	92.01	33.01	91.06	40.32	94.68	23.40
Zero Shot (No Training Required)										
MCM [48]	94.59	32.20	92.25	38.80	90.31	46.20	86.12	58.50	90.82	43.93
EOE [6]	97.52	12.29	95.73	20.40	92.95	30.16	85.64	57.63	92.96	30.09
NegLabel [32]	99.49	1.91	95.49	20.53	91.64	35.59	90.22	43.56	94.21	25.40
OODD [77]	99.36	2.22	95.01	21.49	87.10	44.76	93.27	30.69	93.69	24.79
CLIPScope [20]	99.61	1.29	96.77	15.56	93.54	28.45	91.41	38.37	95.30	20.88
AdaNeg [84]	99.71	0.59	97.44	9.50	94.55	34.34	94.93	31.27	96.66	18.92
CSP [8]	99.60	1.54	96.66	13.66	92.90	29.32	93.86	25.52	95.76	17.51
ANTS	99.69	0.76	98.53	6.50	95.10	27.45	96.38	18.52	97.40	13.31

Table 6. Full results on OpenOOD Benchmark, where ImageNet is adopted as the ID dataset.

Methods	FPR95 ↓		AUROC ↑	
	Near-OOD	Far-OOD	Near-OOD	Far-OOD
Requires Manually Labeled Training Samples				
GEN [47]	–	–	78.97	90.98
AugMix [24] + ReAct [63]	–	–	79.94	93.70
RMDS [59]	–	–	80.09	92.60
AugMix [24] + ASH [14]	–	–	82.16	96.05
Zero Shot (No Training Required)				
MCM [48]	79.02	68.54	60.11	84.77
NegLabel [32]	68.18	27.34	76.92	93.30
EOE [6]	82.93	46.73	66.94	89.14
AdaNeg [83]	67.51	17.31	76.70	96.43
ANTS	60.98	15.38	82.15	96.50

Table 7. Detailed OOD detection results of ANTS on the OpenOOD benchmark, where ImageNet is adopted as the ID dataset.

Near-/Far-OOD		Datasets	FPR95 ↓	AUROC ↑
Near-OOD		SSB-hard	62.73	81.97
		NINCO	59.23	82.32
		Mean	60.98	82.15
Far-OOD		iNaturalist	0.76	99.60
		Textures	16.50	96.78
		OpenImage-O	28.89	93.13
		Mean	15.38	96.50

Table 8. Near OOD detection results.

Method	ImageNet-10 (ID) ImageNet-20 (OOD)		ImageNet-20 (ID) ImageNet-10 (OOD)	
	AUROC \uparrow	FPR95 \downarrow	AUROC \uparrow	FPR95 \downarrow
MCM [48]	98.71	5.00	97.87	17.40
NegLabel [32]	96.86	5.10	96.46	14.60
EOE [6]	99.09	4.20	98.10	13.93
AdaNeg [84]	99.17	3.00	97.25	14.40
ANTS (Ours)	99.56	2.00	98.31	8.90

Table 9. OOD detection results of other instantiations of Adaptive Weighted Score.

Methods	FPR95 \downarrow		AUROC \uparrow	
	Near-OOD	Far-OOD	Near-OOD	Far-OOD
Only ENS	66.23	21.70	77.58	95.81
Only VSNL	62.36	31.15	79.10	92.46
Logarithmic	61.58	21.04	79.60	95.83
Exponential	62.08	22.80	78.98	95.68
Fractional	59.23	19.96	82.32	96.40

Table 10. The robustness of zero-shot OOD detection to domain shift. The ViTb/16 CLIP encoder is used.

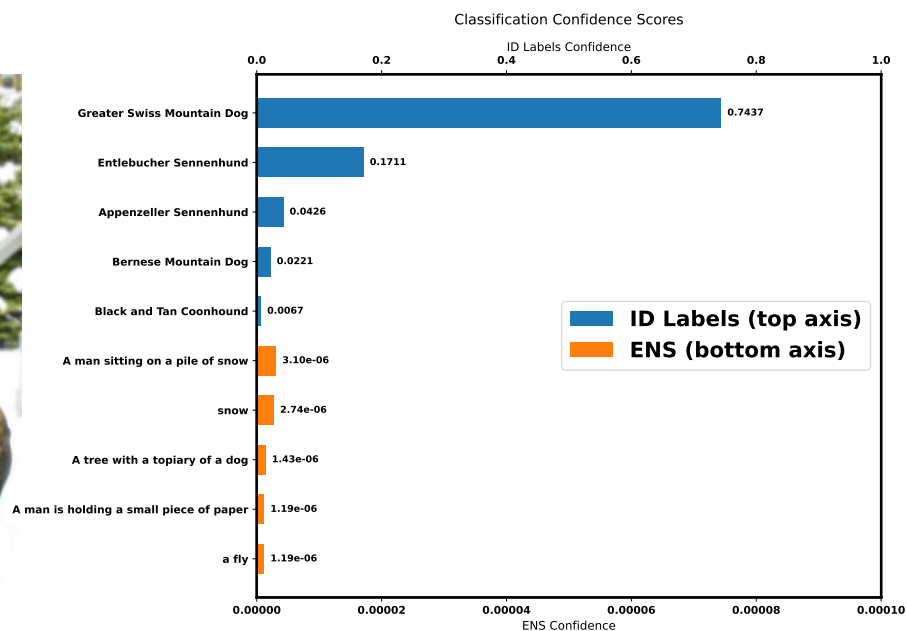
ID Dataset	Methods	OOD datasets									
		INaturalist		SUN		Places		Textures		Average	
		AUROC \uparrow	FPR95 \downarrow	AUROC \uparrow	FPR95 \downarrow	AUROC \uparrow	FPR95 \downarrow	AUROC \uparrow	FPR95 \downarrow	AUROC \uparrow	FPR95 \downarrow
ImageNet-S	MCM	87.74	63.06	85.35	67.24	81.19	70.64	74.77	79.59	82.26	70.13
	NegLabel [32]	99.34	2.24	94.93	22.73	90.78	38.62	89.29	46.10	93.59	27.42
	ANTS (Ours)	99.75	0.80	98.62	6.24	94.17	20.95	93.39	26.08	96.48	13.52
ImageNet-A	MCM [48]	79.50	76.85	76.19	79.78	70.95	80.51	61.98	86.37	72.16	80.88
	NegLabel [32]	98.80	4.09	89.83	44.38	82.88	60.10	80.25	64.34	87.94	43.23
	ANTS (Ours)	98.70	3.55	96.06	21.36	89.38	32.61	93.12	25.55	94.31	20.77
ImageNet-R	MCM [48]	83.22	71.51	80.31	74.98	75.53	76.67	67.66	83.72	76.68	76.72
	NegLabel [32]	99.58	1.60	96.03	15.77	91.97	29.48	90.60	35.67	94.54	20.63
	ANTS (Ours)	99.32	1.31	98.17	10.80	93.80	20.54	94.40	22.84	96.42	13.88
ImageNet-V2	MCM [48]	91.79	45.90	89.88	50.73	86.52	56.25	81.51	69.57	87.43	55.61
	NegLabel [32]	99.40	2.47	94.46	25.69	90.00	42.03	88.46	48.90	93.08	29.77
	ANTS (Ours)	99.50	1.32	98.45	7.98	94.28	22.01	95.93	19.75	97.04	12.77

Table 11. Zero-shot OOD detection performance with different ID datasets. The ViTb/16 CLIP encoder is used.

ID Dataset	Methods	OOD datasets									
		INaturalist		SUN		Places		Textures		Average	
		AUROC \uparrow	FPR95 \downarrow	AUROC \uparrow	FPR95 \downarrow	AUROC \uparrow	FPR95 \downarrow	AUROC \uparrow	FPR95 \downarrow	AUROC \uparrow	FPR95 \downarrow
CUB-200-2011	MCM [48]	98.24	9.83	99.10	4.93	98.57	6.65	98.75	6.97	98.66	7.09
	EOE [6]	99.98	0.07	100.00	0.01	99.92	0.28	100.00	0.00	99.98	0.09
	NegLabel [32]	99.96	0.18	99.99	0.02	99.90	0.33	99.99	0.01	99.96	0.13
	ANTS (Ours)	99.96	0.03	99.99	0.00	99.83	0.02	100.00	0.00	99.95	0.01
STANFORD-CARS	MCM [48]	99.77	0.05	99.95	0.02	99.89	0.24	99.96	0.02	99.89	0.08
	EOE [6]	99.99	0.00	99.99	0.01	99.97	0.11	100.00	0.00	99.99	0.03
	NegLabel [32]	99.99	0.01	99.99	0.01	99.99	0.03	99.99	0.01	99.99	0.01
	ANTS (Ours)	100.00	0.00	100.00	0.00	99.97	0.00	100.00	0.00	99.99	0.00
Food-101	MCM [48]	99.78	0.64	99.75	0.90	99.58	1.86	98.62	4.04	99.43	1.86
	EOE [6]	99.98	0.06	100.00	0.00	99.97	0.14	99.01	2.61	99.74	0.70
	NegLabel [32]	99.99	0.01	99.99	0.01	99.99	0.01	99.60	1.61	99.90	0.40
	ANTS (Ours)	99.99	0.01	100.00	0.00	99.98	0.05	99.72	0.13	99.92	0.05
Oxford-IIIT Pet	MCM [48]	99.38	2.85	99.73	1.06	99.56	2.11	99.81	0.80	99.62	1.70
	EOE [6]	100.00	0.00	99.99	0.01	99.97	0.14	99.97	0.11	99.98	0.07
	NegLabel [32]	99.38	2.85	99.73	1.06	99.56	2.11	99.81	0.80	99.62	1.70
	ANTS (Ours)	100.00	0.00	100.00	0.03	99.97	0.03	99.97	0.00	99.99	0.02



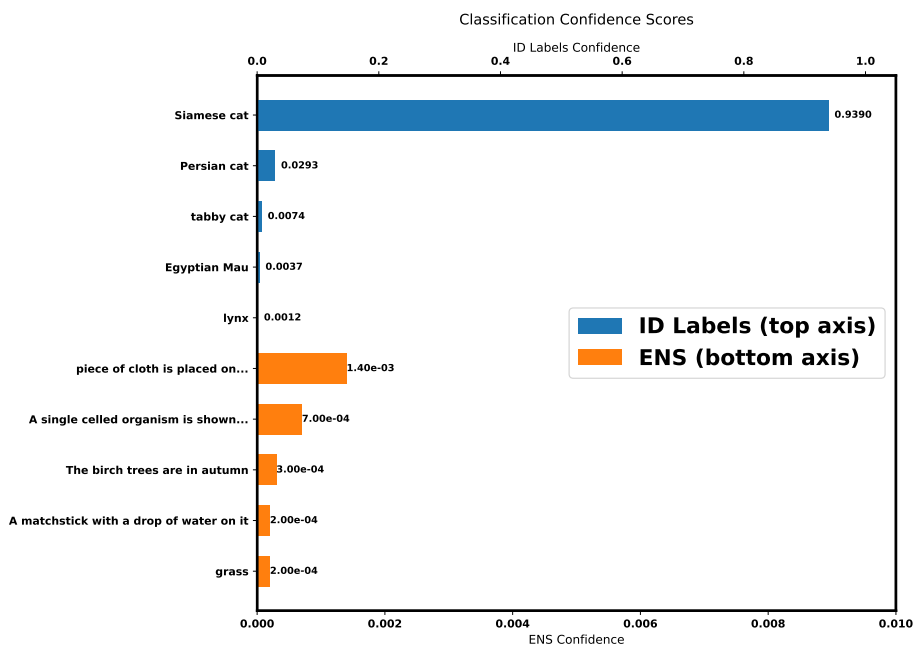
ID Dataset: ImageNet



(a)



ID Dataset: ImageNet

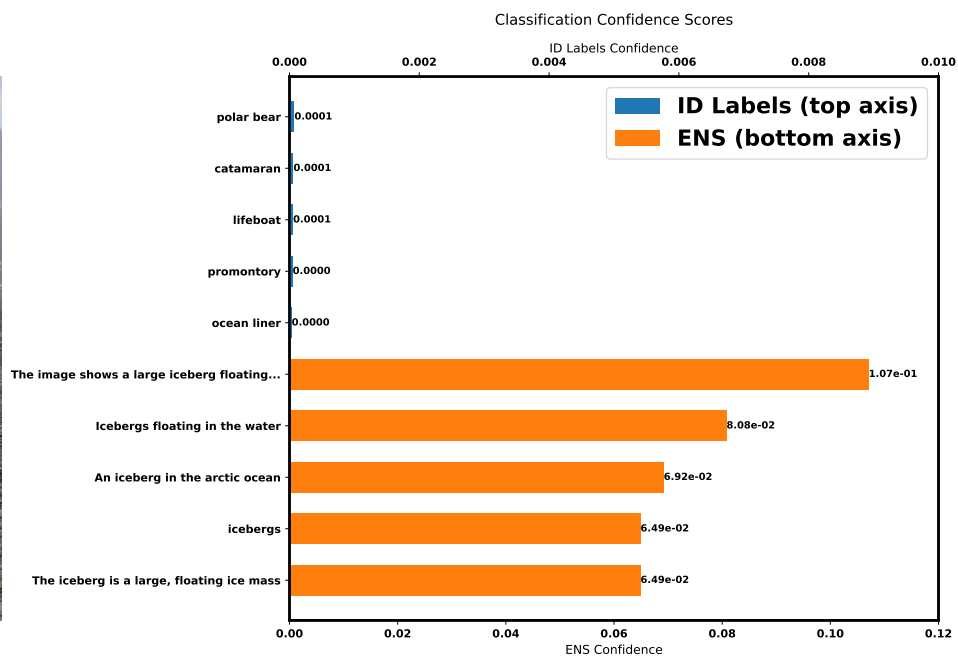


(b)

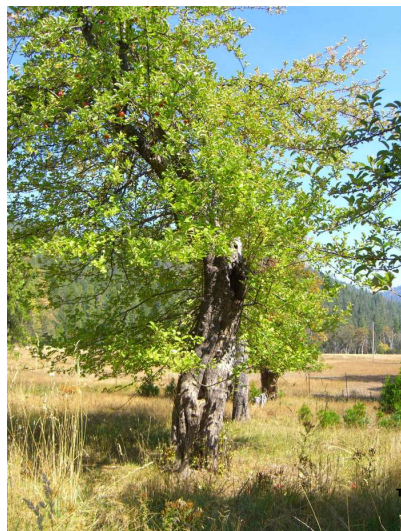
Figure 9. Example cases of classification confidence scores on ImageNet ID samples.



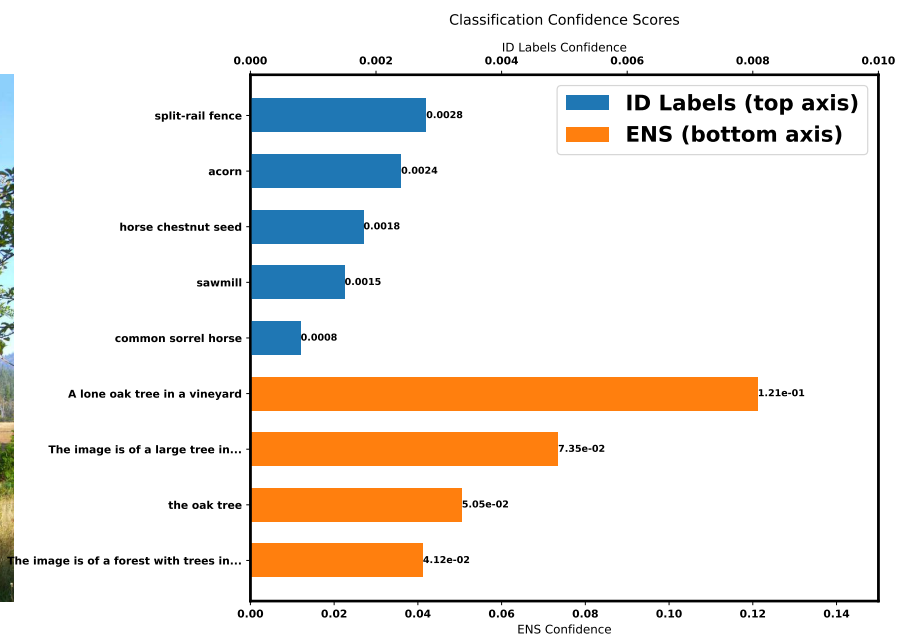
Far-OOD Dataset: SUN



(a)



Far-OOD Dataset: SUN

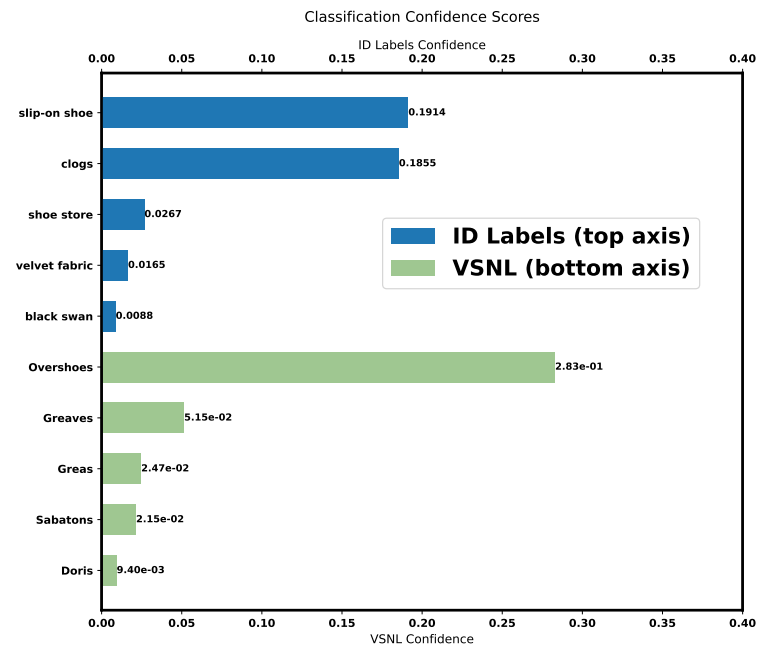


(b)

Figure 10. Example cases of classification confidence scores on Far-OOD samples of the SUN dataset.



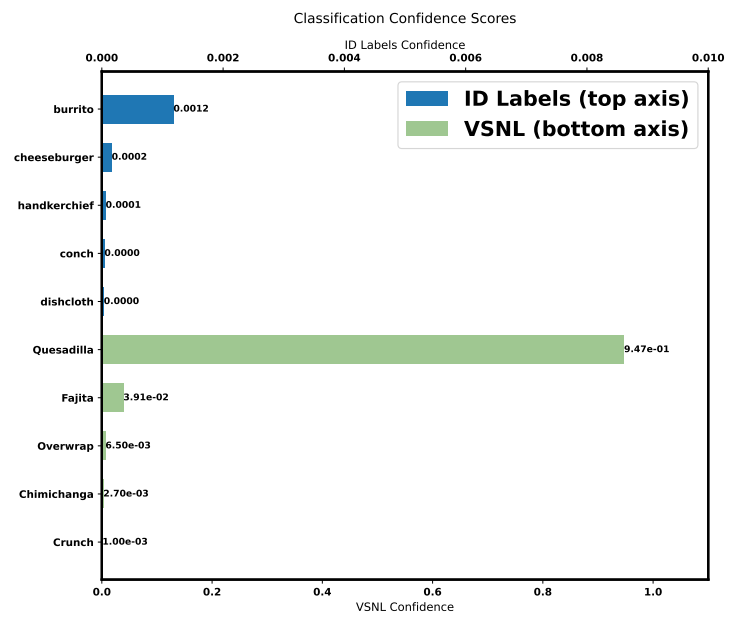
Near-OOD Dataset: NINCO



(a)



Near-OOD Dataset: NINCO



(b)

Figure 11. Example cases of classification confidence scores on Near-OOD samples of the NINCO dataset.